

# Measurement of Electron Temperature Profile and Fluctuation with ECE Radiometer System in Heliotron J<sup>\*)</sup>

Maoyuan LUO, Kazunobu NAGASAKI<sup>1)</sup>, Gavin WEIR<sup>2)</sup>, Hiroyuki OKADA<sup>1)</sup>, Takashi MINAMI<sup>1)</sup>, Shinichiro KADO<sup>1)</sup>, Shinji KOBAYASHI<sup>1)</sup>, Satoshi YAMAMOTO<sup>1,3)</sup>, Shinsuke OHSHIMA<sup>1)</sup>, Tohru MIZUUCHI<sup>1)</sup>, Shigeru KONOSHIMA<sup>1)</sup>, Yuji NAKAMURA and Akihiro ISHIZAWA

*Graduate School of Energy Science, Kyoto University, Uji 611-0011, Japan*

<sup>1)</sup>*Institute of Advanced Energy, Kyoto University, Uji 611-0011, Japan*

<sup>2)</sup>*Max-Planck Institute for Plasma Physics, Greifswald, Germany*

<sup>3)</sup>*Naka Fusion Institute, National Institute and Radiological Science and Technology, Naka 311-0193, Japan*

(Received 6 January 2020 / Accepted 27 April 2020)

A multi-channel electron cyclotron emission (ECE) radiometer system is being developed in Heliotron J to measure electron temperature ( $T_e$ ) profile and evaluate  $T_e$  fluctuation. The conventional ECE part of this system includes 16 channels and can measure electron temperature profile from 58 GHz to 74 GHz which covers from the core to the edge region, and the correlation ECE part is composed of CECE-RF and CECE-IF sides. The signals from these two sides share a same source of electron cyclotron emission and thus are possible to estimate electron temperature fluctuation through correlation analysis. An ECE profile has been obtained and compared with data from Thomson scattering system in an electron cyclotron heated plasma. Electron temperature fluctuation levels were estimated in an ECH plasma using a cross-correlation function and a complex coherence function.

© 2020 The Japan Society of Plasma Science and Nuclear Fusion Research

Keywords: fusion plasma, electron cyclotron emission, correlation ECE, electron temperature fluctuation

DOI: 10.1585/pfr.15.2402038

## 1. Introduction

The study of anomalous transport has become the major topic in the research field of fusion plasma. Measuring electron temperature profile and its fluctuation provides an effective way to study transport and understand turbulence in fusion plasma. Electron cyclotron emission (ECE) is one of the most powerful diagnostics to measure electron temperature. Since Efthimion *et al.* [1] developed a heterodyne radiometry for ECE measurement early in 1979, and multi-channel heterodyne radiometry was developed to measure the electron temperature ( $T_e$ ) profile in a single discharge [2, 3], it has become a common tool for  $T_e$  measurement in modern fusion devices [4]. Local electron temperature in a plasma can be easily obtained by measuring the ECE of certain frequencies. And benefited from the high time resolution of current ECE radiometer system,  $T_e$  fluctuation measurement is also possible [5]. Although correlation ECE radiometers have been developed and applied to some fusion devices for measurement of core  $T_e$  fluctuations [6, 7], study on the role of  $T_e$  fluctuations on energy confinement is still challenging.

In the helical-axis heliotron device, Heliotron J, we have studied effect of the magnetic configuration on global energy confinement [8] and improvement of core heat transport such as internal electron transport barrier (e-ITB)

[9]. Heat transport analysis in the core region is required to understand the physical mechanism of the magnetic configuration effect. For this purpose, we have developed multichannel radiometer systems to measure the  $T_e$  profile and fluctuations. In this paper, we show  $T_e$  profile measurement and first experimental result on  $T_e$  fluctuation using the radiometer in the Heliotron J device. We have adjusted output signal level to obtain more reliable  $T_e$  profile for heat transport analysis. We have also developed a correlation ECE radiometer with wide frequency scan and high accurate frequency setting, which enables us to estimate the correlation of ECE signals.

The organization of this paper is as follow: designing and specification of the ECE radiometer system are shown in section 2; measurement results using conventional and correlation ECE radiometer system are discussed in section 3; summary of this work is in section 4.

## 2. ECE Radiometer System for Heliotron J

Heliotron J is a helical device constructed at the Institute of Advanced Energy of Kyoto University for studying optimization of magnetic configuration in helical device. As the advanced feature of Heliotron J, the basic concept is to reduce neoclassical transport and achieve high beta with small bootstrap current, which carries the potential for developing the currentless ‘quasi-isodynamic’ op-

author's e-mail: [luo.maoyuan.58r@st.kyoto-u.ac.jp](mailto:luo.maoyuan.58r@st.kyoto-u.ac.jp)

<sup>\*)</sup> This article is based on the presentation at the 28th International Toki Conference on Plasma and Fusion Research (ITC28).

timization [10]. The main operation parameters are as follows: major plasma radius: 1.2 m, Average plasma minor radius: 0.1 - 0.2 m, magnetic field strength: 1.5 T, vacuum rotational transform: 0.2 - 0.8, heating systems: electron cyclotron heating (ECH) of up to 0.5 MW, neutral beam injection (NBI) of up to 1.5 MW, and ion cyclotron resonant frequency (ICRF) heating of up to 2.5 MW.

The schematic of the ECE radiometer system for Heliotron J is shown in Fig. 1. The prototype of this radiometer system was firstly designed by Nagasaki *et al.* and upgraded with a correlation part by Weir *et al.* [11]. The radiometer system is composed of two parts, a conventional radiometer part (part A) and a correlation radiometer part (part B). As shown in Fig. 2, the conventional ECE radiometer measures 2nd harmonic X-mode from 58 to 74 GHz with 16 channels, covering the core to the edge region radially. It can be seen that the 2nd harmonic ECE does not overlap with other harmonics. The bandwidth of these channels is 1 GHz. The correlation ECE radiometer part (part B) measures electron temperature fluctuation.

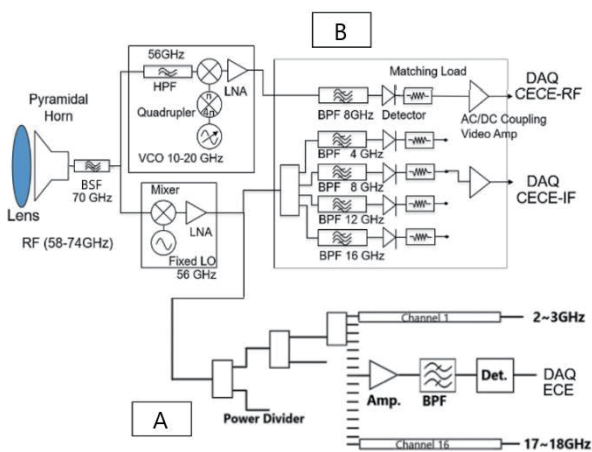


Fig. 1 ECE radiometer system.

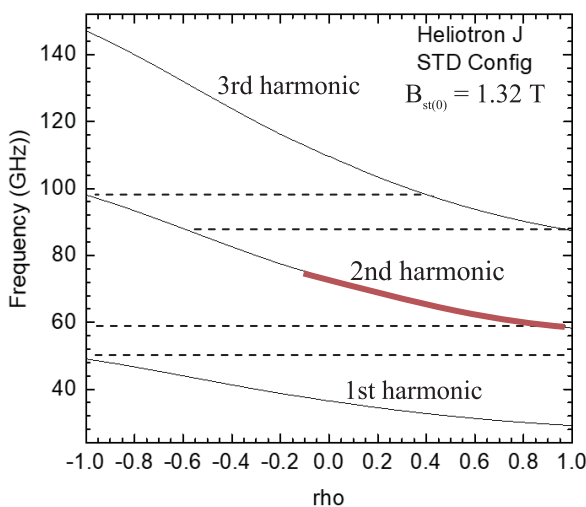


Fig. 2 Radial profiles of electron cyclotron frequency and its harmonics in Heliotron J.

The back end of the correlation radiometer is composed of two sides. The CECE-RF side has a separated front end, which contains a voltage-controlled oscillator (VCO) and a quadrupler allowing flexible RF frequency scan from 56 GHz to 88 GHz with accuracy of 0.1 MHz. The CECE-IF side shares the same front end with the conventional ECE radiometer part, and its back end has 4 frequency-fixed channels of 60 GHz, 64 GHz, 68 GHz and 72 GHz. The bandwidths of these channels are designed and lab tested to be around 200 MHz, which is smaller than the typical scale length of electron temperature fluctuation and should perform a more localized observation.

### 3. Experiment Results

#### 3.1 $T_e$ profile measurement

The conventional ECE radiometer system is relatively calibrated to measure radial profile of electron temperature. The results are compared with Thomson scattering diagnostic results and data near the core is used for cross-calibration. Figure 3 shows a radial profile of electron temperature measured with the ECE radiometer and compared with Thomson scattering diagnostic results. The raw signal intensity in the edge region and core region is adjusted to a similar level within a factor of two in order to obtain the  $T_e$  profile in a wide temperature range. The ECE result agrees well with Thomson result near the core region but has relatively higher values in the edge region. This may be due to low optical thickness at the edge region. Energetic electrons in the inner plasma layers emit frequency downshifted ECE due to relativistic effect, which can be absorbed by outer layer if the plasma is optically thick. In this case the optical depth in the edge ( $\rho > 0.6$ ) drops below 1 according to a ray tracing code, TRAVIS, and thus emissions from inner layers of plasma were not well absorbed and were detected by channels of outer layers, which caused the measured electron temperature higher than real value in the edge region. Multi-pass reflection

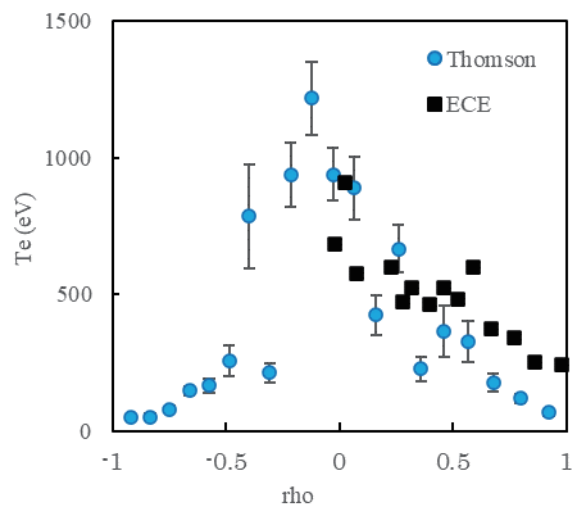


Fig. 3 Radial profile of electron temperature.

from the chamber wall may also affect the measurement.

## 3.2 $T_e$ fluctuation measurement

### 3.2.1 Principle of correlation ECE

In CECE radiometry, the bandwidth of the signal relevant to turbulence is comparable to that of the detection instrument, which leads to a relatively large thermal noise about several percent [12]. The typical amplitude of electron temperature fluctuation associated with anomalous transport is in the order of 1%. Thus, conventional ECE radiometer system is not suitable for measuring  $T_e$  fluctuation [13]. CECE radiometer is a technique to reduce thermal noise. Signals measured by two channels of a CECE radiometer system are coherent with respect to electron temperature fluctuation, but not coherent with respect to thermal noises. Then thermal noise can be reduced by standard correlation analysis techniques.

In this work, two methods are used to estimate electron temperature fluctuation. One is based on cross-correlation function:

$$\frac{\tilde{T}_e}{T_e} = [R_{xy}(\Delta t = 0)]^{1/2} = \langle xy \rangle^{1/2}, \quad (1)$$

where  $R_{xy}$  is the cross-correlation function:

$$R_{xy}(\Delta t) = \langle x(t)y(t + \Delta t) \rangle. \quad (2)$$

The other is based on the complex coherence function:

$$\frac{\tilde{T}_e}{T_e} = \sqrt{\frac{2}{B_{IF}} \int_{f_1}^{f_2} \text{Re}\{\gamma_{xy}(f)\} df}, \quad (3)$$

where  $\gamma_{xy}$  is the complex coherence:

$$\gamma_{xy}(f) = \frac{G_{xy}(f)}{\sqrt{G_{xx}(f)G_{yy}(f)}}, \quad (4)$$

$G_{xy}(f)$  is the cross spectral density as

$$G_{ij}(f) = \langle F_i^*(f)F_j(f) \rangle, \quad (5)$$

where  $F_i$  is the FFT frequency spectrum of one of the channels.

### 3.2.2 Correlation ECE measurement

We measured electron temperature fluctuation with the CECE system in an ECH plasma. The raw signals are shown in Fig. 4 where CECE-RF channel measured  $68.3 \pm 0.1$  GHz and CECE-IF channel measured  $68 \pm 0.1$  GHz. Electron density is set around  $0.7 \times 10^{19} \text{ m}^{-3}$  and ECH power is around 257 KW. In the frequency scan, we fixed one channel to 68 GHz ( $\rho \sim 0.25$ ) and scanned the other channel from 67 GHz to 69 GHz for every 0.1 GHz. The signal contains both electron temperature fluctuation and thermal noise, which will be reduced by correlation analysis.

#### Method one: cross-correlation function

For each frequency separation in the scan, cross-correlation was calculated using cross-correlation function

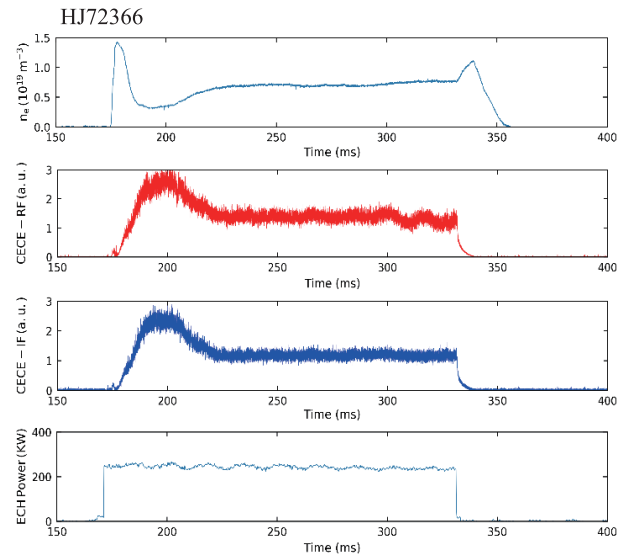


Fig. 4 Time evolution of electron density, CECE signals and ECH power.

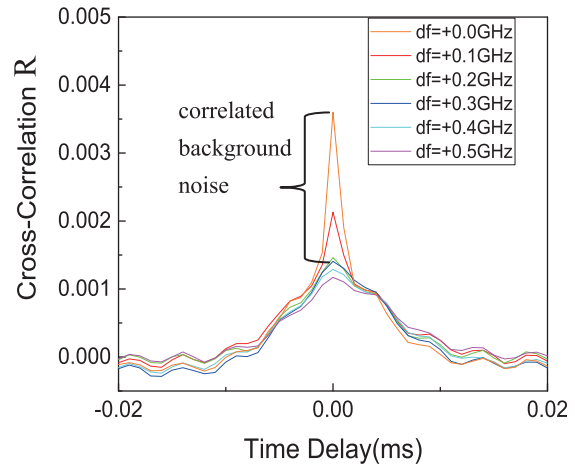


Fig. 5 Cross-correlation in a frequency scan.

shown in previous section. Figure 5 shows the cross correlation from 0 to 0.5 GHz separation. Generally the cross correlation decreases with wider separation. When separation is smaller than 0.2 GHz, a peak appears at zero time-delay. This is due to the overlapping of two channels since their bandwidths are 200 MHz. The overlapping caused the channels to pick up incoherent noise from the same volume which invalidate our assumption that noise is not coherent. Similar phenomenon was also observed in Ref [14], in which these peaks are thought not suitable to represent the actual electron temperature fluctuation. When the separation is larger than 0.4 GHz, the cross correlation reaches a rather stable value, and can be used to estimate electron temperature fluctuation. Figure 6 shows the fluctuation level calculated for each separation. For 0.5 GHz separation, the electron temperature fluctuation level is estimated as 3.8%.

#### Method two: complex coherence function

The same data were also analyzed with a complex

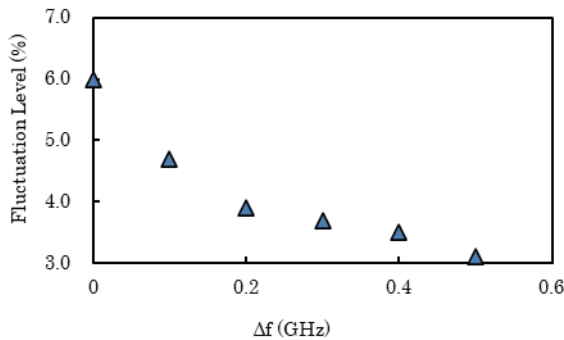


Fig. 6 Electron temperature fluctuation level against separation frequency.

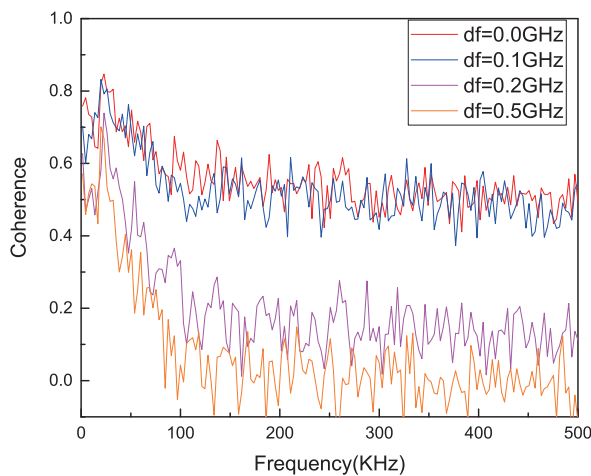


Fig. 7 Coherence of different frequency separations.

coherence function. Coherence was calculated from 0 to 500 KHz for each frequency separation as shown in Fig. 7. In this case, when the frequency separation is large, a peak can be observed around 30 KHz, and when separation decreases below 0.2 GHz, coherence increases in the whole frequency range. This broad band increase of coherence may come from some correlated background noise other than electron temperature fluctuation since they only appear when channels overlap each other. The electron temperature fluctuation levels estimated using complex coherence function with 0 MHz, 100 MHz, 200 MHz, and 500 MHz channel separations are 5.3%, 5.1%, 3.2%, and 1.9% respectively.

The electron temperature fluctuation level obtained by both methods is higher than expected. This may be due to insufficient focusing performance of the lens antenna system. Radial overlapping of the two channels makes the same background noise picked up by both two CECE channels, which invalidates the assumption the noise signals are not correlated. Even when the frequency separation between the two channels is increased beyond the bandwidth of the channels, the focusing performance of the lens antenna system limited the beam width and when the beam is not well enough focused, radial overlapping will happen.

## 4. Summary

We have developed the multi-channel ECE radiometer system in Heliotron J to measure  $T_e$  profile and evaluate  $T_e$  fluctuation. We have adjusted the signal intensity level of 16 channel outputs, which resulted that  $T_e$  profile is available in a wide temperature range. We measured  $T_e$  profile in an ECH plasma with the ECE radiometer system. The results are compared to Thomson scattering diagnostic data and electron temperature in the edge measured by ECE is higher probably due to the effect of energetic electrons. The electron temperature fluctuation levels were also estimated with the CECE radiometer system. The local oscillator of CECE-RF can scan the frequency with high accuracy enough for estimating the correlation. With this CECE radiometer, we have obtained the first experimental results on  $T_e$  fluctuations in Heliotron J. The results might be higher than the real value. This may be due to the focusing performance of the lens. We will improve the focusing performance of the antenna system to achieve localized measurement by replacing the lens into a newly designed one. In future experiment using the developed ECE radiometers, we will evaluate how electron heat transport coefficient and  $T_e$  fluctuation changes in different magnetic configurations and e-ITB plasmas, which could provide us knowledge about the relationship between confinement and turbulence.

## Acknowledgement

The authors are grateful to Heliotron J staff for conducting the plasma experiments. This work was performed with support from and under the auspices of the Collaboration Program of the Laboratory for Complex Energy Processes, IAE, Kyoto University, the NIFS Collaborative Research Program (grant nos. NIFS10KUHL030), the NIFS/NINS project of Formation of International Scientific Base and Network, and Grant-in-Aid for Scientific Research (B) and JSPS Core-to-Core Program, A. Advanced Research Networks.

- [1] P.C. Efthimion *et al.*, Rev. Sci. Instrum. **50**, 949 (1979).
- [2] Y. Nagayama *et al.*, Fusion Eng. Des. **53** (1-4), 201 (2001).
- [3] G. Cima *et al.*, Rev. Sci. Instrum. **56**, 1870 (1985).
- [4] H.J. Hartfuss and M. Tutter, Rev. Sci. Instrum. **56**, 1703 (1985).
- [5] S. Inagaki *et al.*, Phys. Rev. Lett. **107** (11), 115001 (2011).
- [6] S. Sattler *et al.*, Phys. Rev. Lett. **72**, 653 (1994).
- [7] A. White, Phys. Plasmas **15**, 056116 (2008).
- [8] T. Mizuuchi *et al.*, Fusion Sci. Technol. **50**, 352 (2006).
- [9] N. Kenmochi *et al.*, Sci. Rep. **10**, 5 (2020).
- [10] T. Obiki *et al.*, Plasma Phys. Control. Fusion **42**, 11, 1151 (2000).
- [11] G. Weir *et al.*, J. In: EPJ Web of Conf. EDP Sci. (2019) p.03013.
- [12] G. Cima *et al.*, Phys. Plasmas **2**, 720 (1995).
- [13] C. Watts, Fusion Sci. Technol. **52**, 2, 176 (2007).
- [14] A. White, Ph D. thesis, Univ. California, Los Angeles, 2008.